

Cite this: *J. Mater. Chem. C*, 2014, 2, 8546

Influence of the cation type on the DFB lasing performance of dye-doped azobenzene-containing polyelectrolytes†

Leonid M. Goldenberg,^{*a} Victor Lisinetskii,^{*b} Alexander Ryabchun,^{cd} Alexey Bobrovsky^d and Sigurd Schrader^b

The well-known commercially available azobenzene-containing polyelectrolyte poly{1-[4-(3-carboxy-4-hydroxyphenylazo)benzenesulfonamido]-1,2-ethanediyl, sodium salt} (PAZO-Na) has been easily modified by converting it into carboxylic acid and different salts. These new materials, similar to original PAZO-Na, were used as matrices to create DFB lasers based on polarization gratings. Such matrix modification allowed us to obtain laser generation with the laser dye 1,2,3,5,6,7-hexamethyl-8-cyanopyrromethene-difluoroborate complex (pyrromethene 650), to increase the laser device stability (up to a half-life time of 4×10^4 pulses) and to considerably increase the laser efficiency (up to 9%). Therefore, these polymer composites can be considered as cheap and promising materials for photonics, optoelectronics, and sensor applications.

Received 1st July 2014
Accepted 25th August 2014

DOI: 10.1039/c4tc01413h

www.rsc.org/MaterialsC

Introduction

Solid-state organic lasers have a long history of development.² The lasers based on so-called OLED polymers (conjugated polymers used in organic light emitting diodes) are studied with the hope to achieve electrically pumped lasing (see ref. 2c for recent reviews). The easy fabrication and low cost of organic lasers makes them attractive for spectroscopy and sensing applications, particularly for integrated devices.² Distributed feedback (DFB) lasers based on surface relief structures are fabricated with a typical waveguide configuration.² Here nanoimprint lithography is conventionally used for the fabrication of DFB relief structures.^{2c} A disadvantage of the nanoimprint lithography as well as of similar techniques consists in the necessity of the fabrication of a master form for each of the grating periods of interest (and consequently for each desired laser emitting wavelength). The master fabrication is usually performed *via* e-beam or UV-photolithography. In contrast, new

direct writing optical fabrication techniques, where the DFB structure frequency and the emission wavelength can be easily tuned, have been established recently.^{1,3} The application is based on the well-known ability of materials containing azobenzene chromophores to form surface relief (SRG)⁴ and/or polarization gratings.⁵ Many (but not all) azobenzene-containing materials possess this ability for stable photo-induced orientation and consequently for polarization grating inscription.⁴ The efficiency of polarization grating inscription depends on the maximum of the photo-induced birefringence. While materials with a photo-induced birefringence level of up to 0.5 were reported,⁶ even the level of birefringence as small as 0.01 was sufficient to create index gratings functioning as DFB structures for lasing.^{3b} As has already been shown,^{1,3b,d} the polarization gratings in azobenzene-containing materials (side-chain and main-chain polymers, molecular glasses and supramolecular materials)³ have significantly higher potential in comparison with SRGs as DFB structures for lasing due to the sufficiently higher inscription rate. This allows for avoiding or minimizing fluorophore bleaching by the light during the holographic exposure. While SRG was successfully applied by now only to an epoxy oligomer^{3a,c} due to this material's high rate of SRG inscription, polarization gratings were realized in four different azobenzene matrices.^{1,3b,d,f} An exploitation of a wealth of possible azobenzene-containing materials is the route for further improvement of laser performance parameters such as the efficiency, stability and tuning range. The water-soluble polyelectrolyte poly{1-[4-(3-carboxy-4-hydroxyphenylazo)benzenesulfonamido]-1,2-ethanediyl, sodium salt} (PAZO-Na, Fig. 1) is commercially available from Sigma-Aldrich. It contains negatively charged azobenzene moieties in the side chain. The

^aPlasmachem GmbH, Rudower Chaussee 29, 12489 Berlin, Germany. E-mail: lengold57@googlemail.com

^bTechnical University of Applied Sciences Wildau, Hochschulring 1, 15745 Wildau, Germany. E-mail: lisinetskii@gmail.com

^cFraunhofer Institute for Applied Polymer Research, Geiselbergstr. 69, 14476 Potsdam-Golm, Germany

^dFaculty of Chemistry, Moscow State University, Leninskie Gory, Moscow, 119991 Russia

† Electronic supplementary information (ESI) available: Fig. S1: absorbance spectra of the polymer solutions in methanol. Fig. S2: dependence of the normalized lasing wavelength (λ_l/h) on the normalized grating period (A/m) for DFB structures in systems containing different laser dyes in a matrix of PAZO-H. See DOI: 10.1039/c4tc01413h

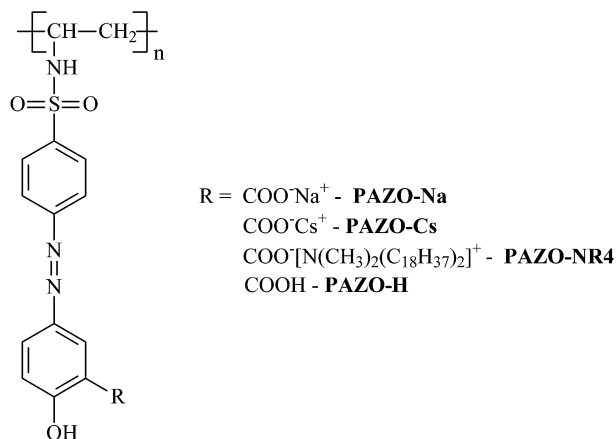


Fig. 1 Chemical formula of the matrix materials: PAZO derivatives.

material has been widely used in recent years for the fabrication of thin films using the so-called electrostatic layer-by-layer procedure.⁷ Photo-induced birefringence has been produced in these films⁸ and they were used for the alignment of liquid crystals.⁹ Also SRG using polarization holographic exposure was produced in these layer-by-layer films.¹⁰ More recently pristine films of the material were used for fabrication of SRGs,^{11a} where also single-beam manipulation^{11b} has been exploited. These materials have also been exploited for the induction of photo-induced birefringence.^{11a} In addition, it was reported that photo-induced birefringence is induced faster at higher pH values.^{8a} Further, the material has been used for different photonic applications including the fabrication of hierarchical structures made of SRGs,¹² spin-coated distributed Bragg reflection mirrors and the corresponding DBR lasers,¹³ and bi-layer distributed feedback (DFB) lasers¹⁴ where the PAZO-Na layer was the layer with DFB structures inscribed. The most interesting photonic application of the PAZO-Na material was found rather recently as the material which has been successfully used for a single layer DFB laser where the emitter (laser dye) and the DFB structure (polarization grating; fabrication of lasers based on SRG in PAZO-Na was not possible due to moderate rates of SRG inscription)^{3a} were both incorporated into a thin layer of the PAZO-Na material.¹ The performance of such devices depends on the ability to induce birefringence by light, the compatibility of the matrix with lasers dyes and the photophysical properties of the dyes in the matrix.

Recently, the use of the azobenzene-containing polyelectrolyte PAZO-Na allowed us to obtain tunable laser radiation in a spectral range from *ca.* 640 to 870 nm with efficiencies of up to 0.7%.¹ This material has the advantage to be commercially available and cheap, and it shows also a sufficient level of photo-induced birefringence of 0.09.¹ Being ionic, the material is strongly polar and soluble in water and alcohols. Doped with the strongly polar Rhodamine dyes and some charged NIR emitting styryl dyes it showed pronounced laser radiation.¹ From the other side, being a salt this material should allow rather simple modification.

In the present paper we demonstrate that a simple modification of the PAZO-Na azobenzene-containing polymer

(converting it into carboxylic acid, and then into ammonium and cesium salts) changes the matrix properties and shows how it affects lasing properties of the dyes.

Experimental part

Film fabrication and characterization

Rhodamine 6G, Rhodamine 610, Rhodamine 640, Kiton Red 620, Rhodamine 700 (LD 700), Rhodamine 800 (LD 800), Pyridine 1, Pyridine 2, DCM, DCM2, pyrromethene 605, pyrromethene 650, LDS 730, LDS 798 and Exalite 613 (all Exciton) laser dyes have been used as received. Poly{1-[4-(3-carboxy-4-hydroxyphenylazo)benzenesulfonamido]-1,2-ethanediyl} (PAZO-Na, Aldrich) has been used as received.

The films were cast or spin-coated onto soda lime glass substrates (refractive index 1.52, Carl Roth GmbH) from 2-methoxyethanol and cyclopentanone solutions for PAZO-Na, PAZO-H, PAZO-Cs and PAZO-NR4, respectively. Laser dyes were introduced into the material as guests (*ca.* 4 wt%) using the same solvents. The dyes employed in this study are depicted in Fig. 2.

Photo-induced birefringence of the materials has been measured with the method described previously.⁵ Film samples were irradiated with linearly polarized radiation of an Ar-ion laser (wavelength 488 nm), which induced a uniaxial

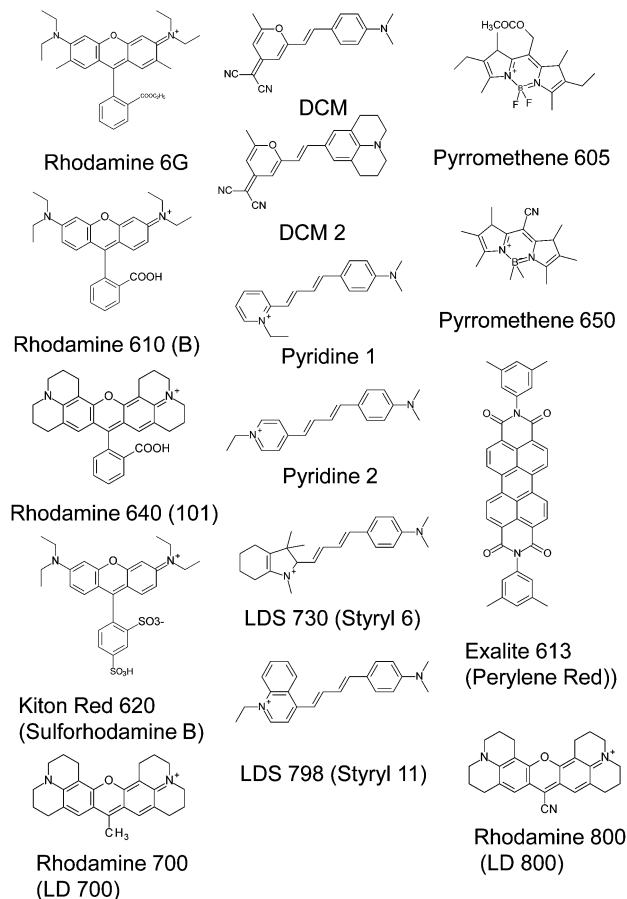


Fig. 2 Chemical formula of the used laser dyes.

birefringence. This birefringence was tested with radiation of a He–Ne laser (wavelength 633 nm) linearly polarized at an angle of 45° with respect to the induced optical axis. Being transmitted through the film, the laser beam polarization was analyzed with a system consisting of a half-wave phase plate, a Glan-prism and a photodetector (Thorlabs DET100A). The induced birefringence (Δn) was estimated according to the following formula:⁵

$$\Delta n = \frac{\lambda_{\text{HeNe}}}{\pi d} \arcsin\left(\sqrt{\frac{I_S}{I_S + I_P}}\right), \quad (1)$$

where I_P and I_S are intensities of transmitted beam components polarized parallel and orthogonal to the polarization of the input beam, respectively, λ_{HeNe} is the wavelength of the probe beam (633 nm), and d is the thickness of the sample. The film thickness was measured using a Veeco Dektak 150 profilometer.

Modification of PAZO-Na

The polymer PAZO-H was prepared as follows: to the solution of PAZO-Na in deionised water (10 wt%) 1.3 equivalent of hydrochloric acid was added dropwise under intense stirring. The precipitated product was filtered off, washed with water until neutral pH and dried at 80 °C overnight. The polymer PAZO-Cs was obtained by neutralization of the acid derivative. A water solution of cesium hydroxide (5 wt%) was slowly added to the suspension of an equimolar amount of PAZO-H in water. During the reaction the formed cesium salt was dissolved. After 24 h of stirring at room temperature the reaction mixture was evaporated and dried in vacuum at 60 °C. The obtained polymer was used for film fabrication without further purification. The polymer PAZO-NR4 was synthesized by cation exchange as follows: to the solution of PAZO-Na in methanol (10 wt%) 1.1 equivalent of the corresponding ammonium salt ($[\text{N}(\text{CH}_3)_2(\text{C}_{18}\text{H}_{37})_2]^+\text{Br}^-$) dissolved in methanol was added dropwise under stirring. The formed PAZO-NR4 was precipitated and then filtered off, washed with methanol several times and dried at room temperature. In all cases described above the yield of reaction was in the range of 90–95%. Absorbance spectra of the obtained polymers are given in the ESI (Fig. S1).†

Structuring

The experimental set-up for inscription of polarization gratings based on Lloyd's mirror interferometer was described previously.^{1,3c} Circularly polarized radiation of an Ar-ion laser with a wavelength (λ_0) of 488 nm and a beam intensity of *ca.* 140 mW cm^{-2} was used for the formation of the polarization interference pattern in a film irradiated from the glass side. The formed grating period (Λ) was controlled by the rotation of Lloyd's interferometer, by setting the angle of light incidence (φ):

$$\Lambda = \frac{\lambda_0}{2 \sin(\varphi)} \quad (2)$$

No additional monitoring of the grating period was carried out. The set of incidence angles in the range of *ca.* 88–27.5° resulted in grating periods of 244.2–530 nm. The accuracy of

grating period determination ($\Delta\Lambda$) was related to the accuracy of incidence angle setting ($\Delta\varphi = \pm 0.25^\circ$) as follows:

$$\Delta\Lambda = \frac{\lambda_0 \cos(\varphi)}{2 \sin^2(\varphi)} \Delta\varphi \quad (3)$$

and was equal to *ca.* ± 4 nm for periods of 530 nm decreasing down to less than ± 0.1 nm for periods of *ca.* 245 nm.

Device characterization

The experimental set-up for device characterization was also described previously.^{1,3} An optic parametric oscillator, OPO (Continuum Surelite OPO Plus) with a pulse duration of 3.5 ns and a repetition rate of 10 Hz, was used as the pump source. A cylindrical lens with a focal length of 40 mm was used to shape the pump beam into a narrow stripe of 5 mm in length and 0.4 mm in width, which was oriented along the grating vector. The pump light was linearly polarized in the direction orthogonal to the grating planes. Linear polarization of pump radiation was also oriented parallel to the grating vector. Spectra of generated light were registered with spectrometers Polytec Berlin AG (models ETA-CS-HL and BRC642E, and the latter was used for measurement of time stability) with a width of the instrument function of 3.5–4 nm and a spectral sampling interval of 1.36 nm. Measurements of the pulse energy of pump radiation and generated radiation were carried out with a calibrated silicon photodetector (Thorlabs DET100A). The DFB gratings were stored and tested generally under ambient conditions.

Results and discussion

The application of the PAZO-Na polyelectrolyte allowed the production of rather stable lasers with tuning ranges over 230 nm (using the depicted palette of laser dyes, Fig. 2) and an efficiency of up to 0.7%.¹

From the other side, being a carboxylic acid salt the PAZO-Na material should allow easy chemical transformation, *e.g.* exchange of the cation and transformation into the carboxylic acid. Such modification will also modify the polymer properties such as the polarity, morphology (possibly a change of free volume) and effective refractive index. The polarity should be changed upon transition from salt to acid, while the refractive index should be drastically changed by the exchange of the sodium cation by a long chain ammonium cation, which has a large content of alkyl chains with a low refractive index contribution. To envisage the morphology change is rather difficult. It is also difficult to predict the change of photo-induced birefringence. Thus we have chosen to make such drastic transformation (Table 1) and investigate how the emitting properties of a number of laser dyes will be influenced.

Upon modification of the PAZO-Na polymer at first the solubility has been changed. The polymer PAZO-NR4 had ceased to be soluble in all solvents characteristic for initial PAZO-Na (DMF, methanol, 2-methoxyethanol, and water), and thus becomes soluble in cyclopentanone. The polymer PAZO-H

Table 1 Performance of different laser (observation of lasing and detected lasing thresholds) dyes in different PAZO based matrices

Dye (pump wavelength)	PAZO-Na ($n = 1.67$) ^{a,1}	PAZO-Cs ($n = 1.67$) ^a	PAZO-NR4 ($n = 1.57$) ^a	PAZO-H ($n = 1.68$) ^a
DCM (532 nm)	—	—	—	—
DCM2 (532 nm)	—	—	—	—
Pyridine 1 (480 nm)	—	—	—	—
Pyridine 2 (532 nm)	—	±	—	—
Rhodamine 6 G (520 nm)	—	—	—	—
Rhodamine 610 (550 nm)	2 (0.57)	—	—	—
Kiton Red 620 (550 nm)	2 (0.57)	>2 (0.57)	±	1.2 (0.34)
Rhodamine 640 (565 nm)	8 (2.3)	±	1.2 (0.34)	±
Rhodamine 700 (595 nm)	1.5 (0.43)	0.4 (0.11) 0.2 (0.06)	0.5 (0.14) 0.15 (0.04)	1.5 (0.43) 0.5 (0.14)
Rhodamine 800 (615 nm)	0.5 (0.14)	1.2 (0.34) 0.6 (0.17)	1.2 (0.34) 0.6 (0.17)	1.2 (0.34)
LDS 798 (570 nm)	0.8 (0.23)	1 (0.29) 0.8 (0.23)	1.5 (0.43) 1.5 (0.43)	1.2 (0.34) 1.2 (0.34)
LDS 730 (605 nm)	0.05 (0.014) 0.025 (0.007)	0.2 (0.06) 0.1 (0.03)	±	1.5 (0.43) 0.1 (0.03)
Pyromethene 605 (550 nm)	—	—	—	—
Pyromethene 650 (580 nm)	—	—	—	1.2 (0.34)
Exalite 613 (575 nm)	—	—	—	—

^a Determined from lasing data. — ASE has not been observed; ± ASE or unstable lasing; values are lasing thresholds in mJ cm⁻² (in MW cm⁻²) for the 2nd order laser; values in bold are lasing thresholds for the 1st order laser.

was insoluble in water. This influences the solubility of laser dyes as most of them are of polar nature, and consequently the compatibility between the dye and the matrix.

Despite a transition from the sodium salt to acid, which should constitute a considerable change of polarity, the behavior of the laser dyes does not change drastically (Table 1). The same dyes exhibited lasing with similar lasing threshold values. The photo-induced birefringence for PAZO-H was about 0.1 which is similar to that of the original PAZO-Na. A significant difference has been found with zwitterionic pyromethene dyes (Fig. 2) only. In the strongly ionic PAZO-Na matrix the emission of the pyromethene dyes was suppressed most probably due to chemical interactions with the matrix and a possible change of the structure¹ despite that boron-dipyromethene (BODIPY) dyes are known for their usually high environment-independent quantum yield^{15a} (however, some exceptions exist^{15b}). In the PAZO-H matrix we were able to detect lasing in pyromethene 650 in the 2nd diffraction order with a moderate lasing threshold (Fig. 3a, Table 1).

Fig. 3 presents lasing spectra obtained for different dyes in the PAZO-H matrix. A relatively large width (4–6 nm) of detected lines can be explained with a low resolution of the used spectrometer. Lasing polarization was linear with the orientation corresponding to the TE-mode of the laser waveguides. The lasing wavelength (λ_L) was controlled by inscription of the diffraction grating with a corresponding period (A) according to the Bragg condition:

$$n_{\text{eff}}(\lambda_L) \frac{A}{mh} = \frac{1}{2} \frac{\lambda_L}{h}, \quad (4)$$

where m is the order of diffraction providing laser feedback and n_{eff} is the effective refractive index, which is a solution of the corresponding characteristic equation for the TE-mode:³

$$2\pi \frac{1}{\lambda_L/h} \sqrt{n^2 - n_{\text{eff}}^2} - l\pi = \arctan \left(\sqrt{\frac{n_{\text{eff}}^2 - n_1^2}{n^2 - n_{\text{eff}}^2}} \right) + \arctan \left(\sqrt{\frac{n_{\text{eff}}^2 - n_2^2}{n^2 - n_{\text{eff}}^2}} \right) \quad (5)$$

where h is the thickness of the guiding layer, l is an integer number, and n , n_1 , and n_2 are refractive indices of the guiding layer, of air ($n_1 = 1$), and of the glass substrate ($n_2 = 1.52$), respectively.

Fig. 3 shows that using different dyes and setting a corresponding grating period we were able to obtain lasing with a wavelength between *ca.* 655 and 825 nm. Taking into account that the behavior of dyes in PAZO-H is similar to that for PAZO-Na (Table 1) we can assume that the available tuning range for the PAZO-H matrix is similar to that of the original PAZO-Na polyelectrolyte,¹ however the investigation of the tuning range was out of the scope of this work.

Lasing spectra presented in Fig. 3a were obtained for 2nd order DFB lasers ($m = 2$). For four NIR dyes (Rhodamine 700, Rhodamine 800, LDS 730 and LDS 798) emitting in the longer wavelength side of the spectrum we were able to write also gratings, which produce lasing in the 1st order ($m = 1$) of diffraction. These 1st order DFB lasers have a sufficiently lower generation threshold than the 2nd order lasers (Table 1). Their generation spectra are plotted in Fig. 3b.

Using the experimental data of lasing wavelengths we were able to estimate the refractive index of PAZO-H. Indeed, eqn (4) and (5) show that the dependence of the normalized lasing wavelength (λ_L/h) on the normalized grating period (A/mh) is defined by the refractive index of the guiding layer only (refractive indices of the substrate and air are known). This dependence for experimental data obtained for PAZO-H-based DFB lasers is presented in Fig. S2 in the ESI.† Fitting of this dependence with eqn (4) and (5) yields the value of the refractive index for PAZO-H equal to 1.68 (Table 1), which is rather close to

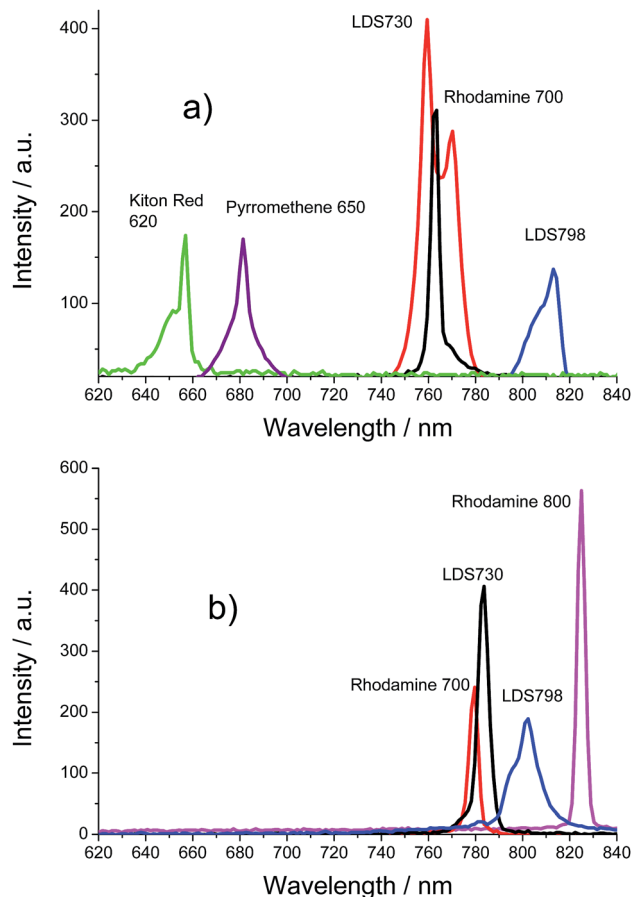


Fig. 3 Lasing spectra of different DFB structures in systems containing different laser dyes (ca. 3–6% w/w) in a matrix of PAZO-H: (a) 2nd order lasing: Kiton Red 620, grating period is 415 nm, film thickness is 320 nm, and pump energy density is 2.2 mJ cm^{-2} ; Pyromethene 650, grating period is 435 nm, film thickness is 320 nm, and pump energy density is 2.8 mJ cm^{-2} ; Rhodamine 700, grating period is 490 nm, film thickness is 400 nm, and pump energy density is 1.6 mJ cm^{-2} ; LDS 798, grating period is 520 nm, film thickness is 320 nm, and pump energy density is 2.2 mJ cm^{-2} ; LDS 730, grating period is 495 nm, film thickness is 320 nm, and pump energy density is 2.4 mJ cm^{-2} ; and (b) 1st order lasing: Rhodamine 700, grating period is 250 nm, film thickness is 320 nm, and pump energy density is 0.7 mJ cm^{-2} ; LDS 730, grating period is 255 nm, film thickness is 250 nm, and pump energy density is 0.7 mJ cm^{-2} ; Rhodamine 800, grating period is 270 nm, film thickness is 250 nm, and pump energy density is 2.4 mJ cm^{-2} ; LDS 798, grating period is 254 nm, film thickness is 400 nm, and pump energy density is 1.8 mJ cm^{-2} .

that of the original PAZO-Na salt form (1.67).^{1,14} Thus the matrices PAZO-Na and PAZO-H appeared to be similar to some differences in polarity and solubility.

The exchange of the sodium cation against cesium or substituted ammonium (Table 1 and Fig. 4 and 5) should not change polarity significantly but might change the refractive index of the polymer due to the change of composition, apparently to the higher and lower values, respectively. The refractive index has been determined from the lasing wavelength data (Fig. 4 and 5) using the same procedure as was described for PAZO-H. It was found that the refractive index for

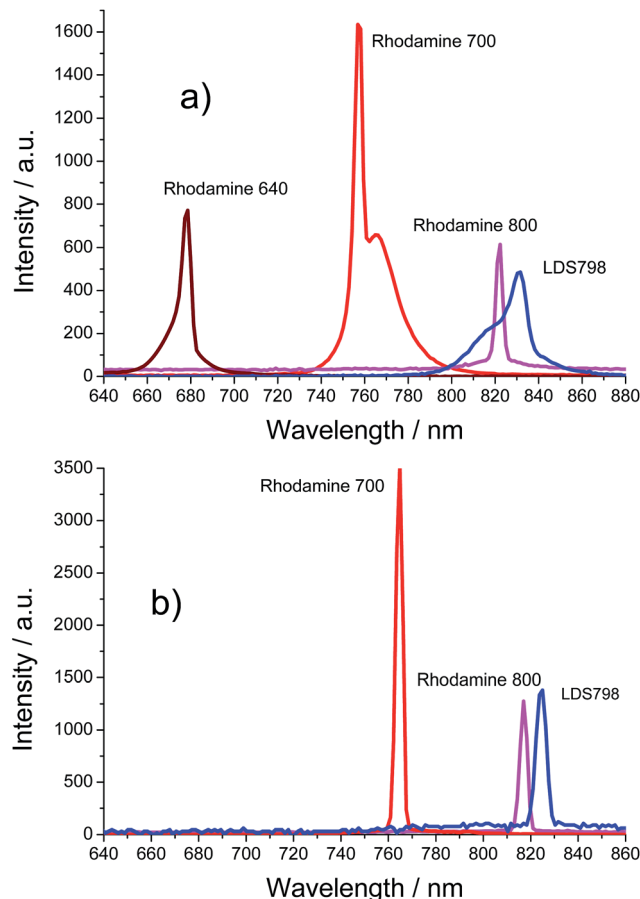


Fig. 4 Lasing spectra of different DFB structures in systems containing different laser dyes (ca. 3–5% w/w) in a matrix of PAZO-NR4: (a) 2nd order lasing: Rhodamine 640, grating period 425 nm, film thickness is $20 \mu\text{m}$, and pump energy density is 1.3 mJ cm^{-2} ; Rhodamine 700, grating period is 480 nm, film thickness is $7 \mu\text{m}$, and pump energy density is 1.1 mJ cm^{-2} ; Rhodamine 800, grating period is 520 nm, film thickness is $4 \mu\text{m}$, and pump energy density is 1.5 mJ cm^{-2} ; LDS 798, grating period 530 nm, film thickness is $17 \mu\text{m}$, and pump energy density is 2.2 mJ cm^{-2} ; and (b) 1st order lasing: Rhodamine 700, grating period is 244 nm, film thickness is $7 \mu\text{m}$, and pump energy density is 0.2 mJ cm^{-2} ; Rhodamine 800, grating period is 260 nm, film thickness is $4 \mu\text{m}$, and pump energy density is 1.1 mJ cm^{-2} ; LDS 798, grating period 263 nm, film thickness is $17 \mu\text{m}$, and pump energy density is 2.2 mJ cm^{-2} .

the cesium salt (1.67, Table 1) was almost the same as that for the sodium salt, while the refractive index of the ammonium salt was sufficiently lower (1.57, Table 1). Thus an introduction of a cation with a high content of alkyl group could be the way to lower the refractive index and consequently to shift the lasing wavelength for the same dye hypsochromically. Photo-induced birefringence has been measured to be 0.06 and 0.01 for PAZO-Cs and PAZO-NR4, respectively. Lower photoinduced birefringence for PAZO-NR4 could be tentatively attributed to the lower content of azobenzene moieties.

From the other point of view both newly synthesized salts (with cesium and ammonium) have shown similar lasing behavior to the same dyes. Emission between 670 and 830 nm with an ammonium salt matrix and emission between 650 and

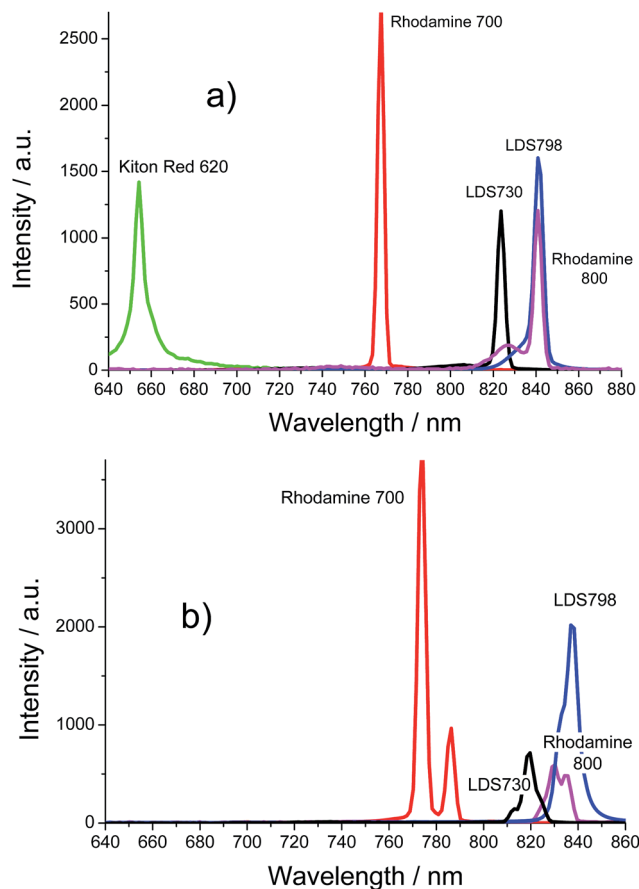


Fig. 5 Lasing spectra of different DFB structures in systems containing different laser dyes (ca. 4–5% w/w) in a matrix of PAZO-Cs: (a) 2nd order lasing: Kiton Red 620, grating period 396 nm, film thickness is 540 nm, and pump energy density is 2.8 mJ cm^{-2} ; Rhodamine 700, grating period is 474 nm, film thickness is 530 nm, and pump energy density is 1.1 mJ cm^{-2} ; LDS 730, grating period is 511 nm, film thickness is 540 nm, and pump energy density is 1.1 mJ cm^{-2} ; LDS 798, grating period 520 nm, film thickness is 540 nm, and pump energy density is 1.3 mJ cm^{-2} ; Rhodamine 800, period 520 nm, film thickness is 520 nm, and pump energy density is 1.5 mJ cm^{-2} ; and (b) 1st order lasing: Rhodamine 700, grating period is 245 nm, film thickness is 530 nm, and pump energy density is 0.7 mJ cm^{-2} ; Rhodamine 800, grating period is 260 nm, film thickness is 520 nm, and pump energy density is 1.2 mJ cm^{-2} ; LDS 798, grating period 260 nm, film thickness is 540 nm, and pump energy density is 1.2 mJ cm^{-2} ; LDS 730, period 255 nm, film thickness is 540 nm, and pump energy density is 0.7 mJ cm^{-2} .

840 nm with a cesium salt matrix have been detected. For both matrices and for all NIR emitting dyes used in this work (Rhodamine 700 and 800, LDS 730 and 798) we were able to fabricate 1st order DFB lasers revealing lower lasing thresholds.

Fig. 6a together with Table 1 shows the obtained lasing thresholds for different laser dyes in different matrices. It can be seen that the lowest threshold was obtained for LDS 730 in PAZO-H and PAZO-Cs matrices. Nevertheless, this threshold (0.1 mJ cm^{-2}) was ca. two times higher than the threshold for LDS 730 in the PAZO-Na matrix (0.05 mJ cm^{-2}).¹ In addition, the generation efficiency of this fluorophore in PAZO-H and PAZO-Cs matrices was considerably lower than that in the PAZO-Na matrix. Dependencies of the generation efficiency for 1st order

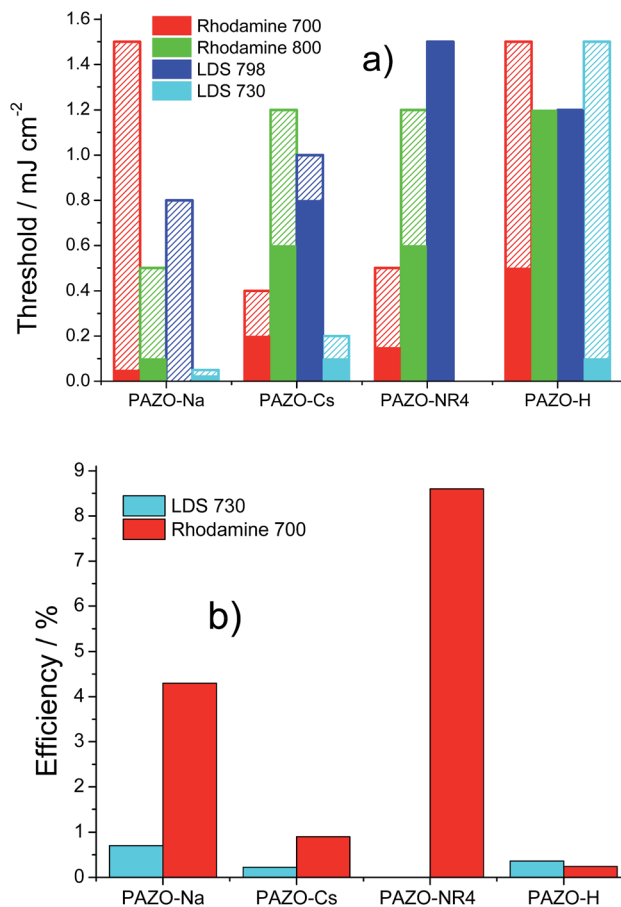


Fig. 6 Dependence of the lasing threshold (a) and the maximum total generation efficiency (b) on the cation type for different laser dyes; (a) filled without pattern bars correspond to 1st order DFB lasers, while filled with pattern bars correspond to 2nd order DFB lasers; and (b) bars are plotted for 1st order DFB lasers; data for the PAZO-Na matrix were taken from ref. 1.

DFB lasers based on LDS 730 in PAZO-H and PAZO-Cs are plotted in Fig. 7a, while the comparison of maximum achieved lasing efficiencies for these lasers is shown in Fig. 6b. The output energy was detected from one edge of a device. As such 1st order DFB lasers emit from two edges, we assumed that the same energy was emitted from the other edge too. Under this assumption the generation efficiency was calculated.

Fig. 6 and 7 show that neither PAZO-H nor PAZO-Cs matrices have an advantage for LDS 730 compared to the PAZO-Na matrix. However, the PAZO-Cs and PAZO-NR4 matrices provide sufficiently high lasing efficiencies for Rhodamine 700. This fluorophore possesses several times higher thresholds than thresholds for LDS 730, but its lasing efficiency (0.9%) in PAZO-Cs is higher than the efficiency (0.7%) of LDS 730 in PAZO-Na. The application of a thick film (thickness is $7 \mu\text{m}$) of Rhodamine 700 in PAZO-NR4 for the fabrication of a 1st order DFB laser resulted in an extremely high total lasing efficiency (8.6%), which is one order of magnitude higher than the efficiency of LDS 730 in PAZO-Na (0.7%) and several times higher than our best previous result (3%) for Rhodamine 700 in the P1 side-chain azobenzene polymer.^{3d}

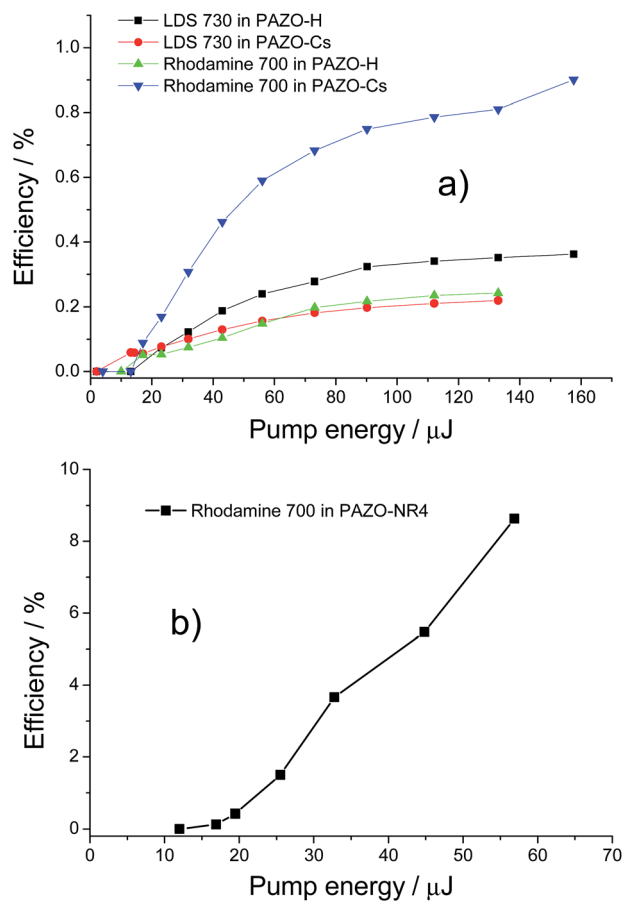


Fig. 7 Lasing efficiency versus pump energy for the lasers emitting in the 1st diffraction order: (a) Rhodamine 700 (ca. 3–5% w/w) in PAZO-H (thickness is 0.32 μm) and in PAZO-Cs (thickness is 0.5 μm), LDS 730 (ca. 3–5% w/w) in PAZO-H (thickness is 0.25 μm) and in PAZO-Cs (thickness is 0.5 μm); (b) Rhodamine 700 (ca. 3–5% w/w) in PAZO-NR4, film thickness is 7 μm (Rhodamine 700).

The duration of pulses generated in the investigated DFB structures was varied from 0.6 ns (close to generation threshold) up to 3 ns (far from the threshold).

The time stability of lasers based on LDS 730 and Rhodamine 700 in different matrices was almost the same. Fig. 8 shows, as an example, time decays of the lasing energy for 1st order DFB lasers based on Rhodamine 700 in PAZO-NR4 and LDS 730 in PAZO-H. The fitting of experimental data provides a half-life of 4×10^4 pulses, which is slightly higher than observed in the original PAZO-Na matrix.¹ We think that the reason for the time decay of lasing is the destruction of dyes, because similar strong degradation of ASE has been also observed. The investigations of the generation efficiency and time stability have been performed only for the 1st order DFB lasers, due to their higher attractiveness (sufficiently lower thresholds (Table 1 and Fig. 6a) and higher efficiencies).¹ However, because lasing degradation is caused by the dye destruction, we can expect that the time decay of 2nd order lasers of the same order as that for 1st order lasers at a given pump.

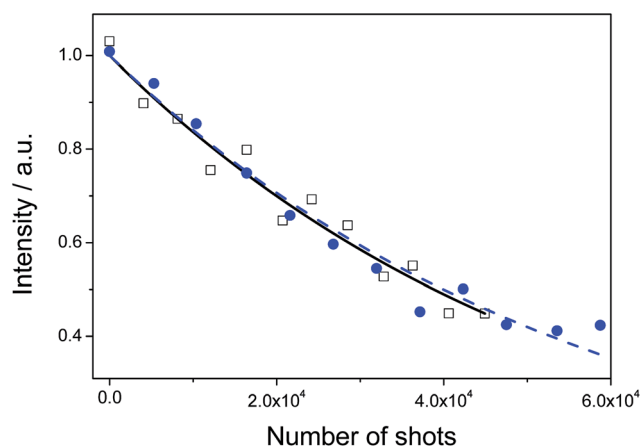


Fig. 8 Dependence of the lasing signal energy on the number of pulses for the laser emitting in the 1st diffraction order in LDS 730 in a PAZO-H matrix (open squares) and Rhodamine 700 in a matrix of PAZO-NR4 (filled circles). The solid and dashed curves are fitted to the experimental data with an exponential decay function, and the fitted curves in both cases have a half-life of ca. 4×10^4 shots. The pump energy was 24 μJ (the energy density was 1.2 mJ cm⁻²).

Conclusions

Easy modification of the azobenzene-containing polyelectrolyte PAZO-Na has been carried out. This allows changing polarity, refractive index and morphology of the polymer matrix used for the fabrication of single layer DFB lasers based on orientation holographic gratings. By matrix modification and laser dye variation a significant change in the properties of laser devices has been observed. Laser generation with the BODIPY dye pyromethene 650 has been detected in the PAZO-H matrix, which can be attributed to lower polarity. The use of the PAZO-NR4 matrix with the dye Rhodamine 700 allowed the laser generation with a lasing efficiency of 8.6%, which is about three times higher than our best previous result.^{3d}

Acknowledgements

This research was supported by the Alexander von Humboldt Foundation and the Russian Foundation of Fundamental Research (13-03-00648, 13-03-12071 and 13-03-12456).

Notes and references

- 1 L. M. Goldenberg, V. Lisinetskii and S. Schrader, *Adv. Opt. Mater.*, 2013, **1**, 768.
- 2 (a) S. Chenais and S. Forget, *Polym. Int.*, 2012, **61**, 390; (b) C. Grivas and M. Pollnau, *Laser Photonics Rev.*, 2012, **6**, 419; (c) I. D. W. Samuel and G. A. Turnbull, *Chem. Rev.*, 2007, **107**, 1272; (d) A. Costela, I. García-Moreno and R. Sastre, *Solid-State Dye Lasers*, in *Tunable Laser Applications*, ed. F.J. Duarte, CRC Press, Boca Raton, USA, 2009, p. 97; (e) L. Xin, S. Panagiotis, B. Wang, T. Woggon, T. Mappes and U. Lemmer, *Opt. Express*, 2013, **21**, 28941.

- 3 (a) L. M. Goldenberg, V. Lisinetskii, Y. Gritsai, J. Stumpe and S. Schrader, *Adv. Mater.*, 2012, **24**, 3339; (b) L. M. Goldenberg, V. Lisinetskii, Y. Gritsai, J. Stumpe and S. Schrader, *Laser Phys. Lett.*, 2013, **10**, 085804; (c) L. M. Goldenberg, V. Lisinetskii and S. Schrader, *Adv. Opt. Mater.*, 2013, **1**, 527; (d) L. M. Goldenberg, V. Lisinetskii and S. Schrader, *Adv. Opt. Mater.*, 2014, **2**, 286; (e) L. M. Goldenberg, V. Lisinetskii and S. Schrader, *Laser Phys.*, 2014, **24**, 035807; (f) L. M. Goldenberg, V. Lisinetskii, A. Ryabchun, A. Bobrovsky and S. Schrader, *ACS Photonics*, 2014, DOI: 10.1021/ph500183n.
- 4 *Azobenzene-containing Polymers and Liquid Crystals*, ed. Y. Zhao and T. Ikeda, Wiley&Sons, Hoboken, NJ, USA, 2009.
- 5 L. Nikolova and P. S. Ramanujam, in *Polarization Holography*, Cambridge Academic Press, Cambridge, UK, 2009.
- 6 (a) K. Okano, A. Shishido and T. Ikeda, *Adv. Mater.*, 2006, **18**, 523; (b) B. L. Lachut, S. A. Maier, H. A. Atwater, M. J. A. de Dood, A. Polman, R. Hagen and S. Kostromine, *Adv. Mater.*, 2004, **16**, 1746; (c) F.-K. Bruder, R. Hagen, T. Rölle, M.-S. Weiser and T. Fäcke, *Angew. Chem., Int. Ed.*, 2011, **50**, 4552.
- 7 (a) Y. Lvov, S. Yamada and T. Kunitake, *Thin Solid Films*, 1997, **300**, 107; (b) S. Dante, R. C. Advincula, C. W. Frank and P. Stroeve, *Langmuir*, 1999, **15**, 193; (c) M.-K. Park and R. C. Advincula, *Langmuir*, 2002, **18**, 4532; (d) S. M. Johal, B. H. Ozer, J. L. Casson, A. St. John, J. M. Robinson and H.-L. Wang, *Langmuir*, 2004, **20**, 2792; (e) J. L. Casson, H.-L. Wang, J. B. Roberts, A. N. Parikh, J. M. Robinson and M. S. Johal, *J. Phys. Chem. B*, 2002, **106**, 1697.
- 8 (a) Q. Ferreira, P. J. Gomes, M. Raposo, J. A. Giacometti, O. N. Oliveira Jr and P. A. Ribeiro, *J. Nanosci. Nanotechnol.*, 2007, **7**, 2659; (b) Q. Ferreira, P. A. Ribeiro, O. N. Oliveira Jr and M. Raposo, *ACS Appl. Mater. Interfaces*, 2012, **4**, 1470.
- 9 (a) M.-K. Park and R. C. Advincula, *Langmuir*, 2002, **18**, 4532; (b) A. Bobrovsky, A. Ryabchun and V. Shibaev, *J. Photochem. Photobiol., A*, 2011, **218**, 137.
- 10 A. Baba, C. Jiang, K.-M. Park, J.-Y. Park, H.-K. Shin and R. Advincula, *J. Phys. Chem. B*, 2006, **110**, 17309.
- 11 (a) L. M. Goldenberg, O. Kulikovska and J. Stumpe, *Langmuir*, 2005, **21**, 4794; (b) Y. Gritsai, L. M. Goldenberg and J. Stumpe, *Opt. Express*, 2011, **19**, 18687.
- 12 (a) L. M. Goldenberg, Y. Gritsai, O. Kulikovska and J. Stumpe, *Opt. Lett.*, 2008, **33**, 1309; (b) Y. Gritsai, L. M. Goldenberg, O. Kulikovska, O. Sakhno and J. Stumpe, *Proc. SPIE*, 2010, **7716**, 77161V.
- 13 L. M. Goldenberg, V. Lisinetskii and S. Schrader, *Laser Phys. Lett.*, 2013, **10**, 055808.
- 14 L. M. Goldenberg, V. Lisinetskii, Y. Gritsai, J. Stumpe and S. Schrader, *Opt. Mater. Express*, 2012, **2**, 11.
- 15 (a) A. Loudet and K. Burgess, *Chem. Rev.*, 2007, **107**, 4891; (b) M. K. Kuimova, G. Yahioglu, J. A. Levitt and K. Suhling, *J. Am. Chem. Soc.*, 2008, **130**, 6672.